

# Self-assembling Depsipeptides on Aggregation-Induced Emission Luminogens: A New Way to Create Programmable Nanovesicles and Soft Nanocarriers

Carla Hernando-Muñoz, Andrea Revilla-Cuesta, Irene Abajo-Cuadrado, Camilla Andreini, Tomás Torroba,\* Natalia Busto,\* Darío Fernández, German Perdomo, Gerardo Acosta, Miriam Royo, Javier Gutierrez Reguera, Angelo Spinello, Giampaolo Barone, Dominic Black, and Robert Pal

Cite This: *ACS Appl. Mater. Interfaces* 2025, 17, 10097–10107

Read Online

ACCESS |

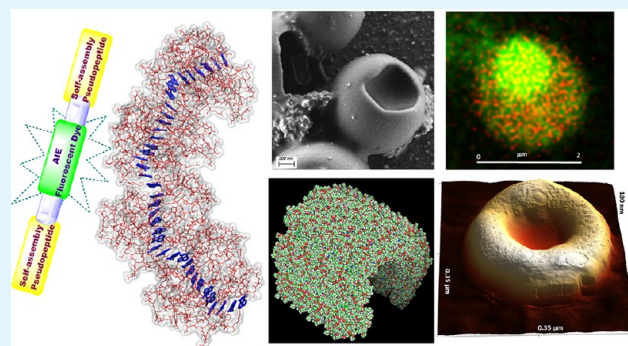
Metrics & More

Article Recommendations

Supporting Information

**ABSTRACT:** We introduce the proof of concept of a new methodology to produce robust hollow nanovesicles stable in water or mixtures of water and organic solvents. The bottom-up produced nanovesicles are formed by the self-assembly of depsipeptide chains of natural origin combined with new aggregation-induced emission luminogens that function as constitutional vesicle-forming moieties and fluorescent indicators of the structure of the nanovesicle. The newly formed nanovesicles are robust enough to be used to carry large molecules such as physiological peptides without losing their structural characteristics, acting as programmable nanocarrier systems within living cells as Trojan horse systems, constituting a new approach to active transport and nanoencapsulation.

**KEYWORDS:** fluorescent materials, aggregation induced emission materials, active transport, nanoencapsulation, programmed cytotoxicity



## INTRODUCTION

The creation of soft nanoparticles using bottom-up nanotechnological methods is an increasingly important demand in our society. Semiconducting and metallic nanocrystals<sup>1</sup> are well suited for established applications such as photonics, catalysis, sensing, energy harvesting and conversion, or bioimaging, and perovskite quantum dots<sup>2</sup> have been applied to solar cells, photocatalysis, emitting devices of light and screens, but all of them have problems such as toxicity, environmental and sustainability problems.<sup>3</sup> Soft organic nanoparticles are much more sustainable and suitable for applications not solved by their metal counterparts. Soft nanoparticle research is highly oriented toward lipid nanoparticles that mimic biological vesicles,<sup>4</sup> such as the development of lipid nanoparticle-based mRNA vaccines for nucleic acid delivery during COVID-19 pandemics.<sup>5</sup> The poor long-term stability of lipid nanoparticles has directed the field toward polymeric<sup>6</sup> or multicomponent nanoparticles.<sup>7</sup> The most important objectives of artificial vesicles are drug/nucleic acid delivery, reaction promoters and regulators, photodynamic therapy, enzyme catalysis mimetics (metallo-nanozymes or photoreactive catalysts), fluorescence imaging, and control or cancer diagnostics. Peptides are suitable due to their intrinsic characteristics of self-assembly and biocompatibility for some of the above uses,<sup>8</sup> but vesicle formation has been

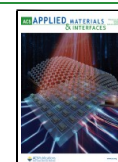
mainly related to amphiphilic peptides<sup>9</sup> and pseudopeptides<sup>10</sup> as functional materials.<sup>11</sup> There is an urgent need for new stable artificial vesicles that can meet the requirements such as cancer therapy.<sup>12</sup> There has been great interest in the chemistry of peptide-based supramolecular systems to access complex functions that arise when multiple interactions are coordinated and integrated<sup>13</sup> and as enzyme mimics or regulators.<sup>14,15</sup> The improvement of precision medicines and the way they can be addressed are largely mediated by innovative drug delivery systems.<sup>16</sup> On the other hand, aggregation-induced emission luminogens (AIEgens)<sup>17</sup> have expanded the field of aggregation-based nanomaterials<sup>18</sup> and are also useful for phototheranostics,<sup>19</sup> super-resolution imaging<sup>20</sup> or smart aggregates in clinical diagnosis.<sup>21</sup> The fusion of peptides and AIE-gens has opened new avenues in biomedicine,<sup>22</sup> drug delivery,<sup>23</sup> and encapsulation of anticancer drugs.<sup>24</sup> The disadvantage of the methodology is that peptides are easily recognized by degradation systems within cells, so

Received: November 5, 2024

Revised: January 20, 2025

Accepted: January 21, 2025

Published: January 31, 2025



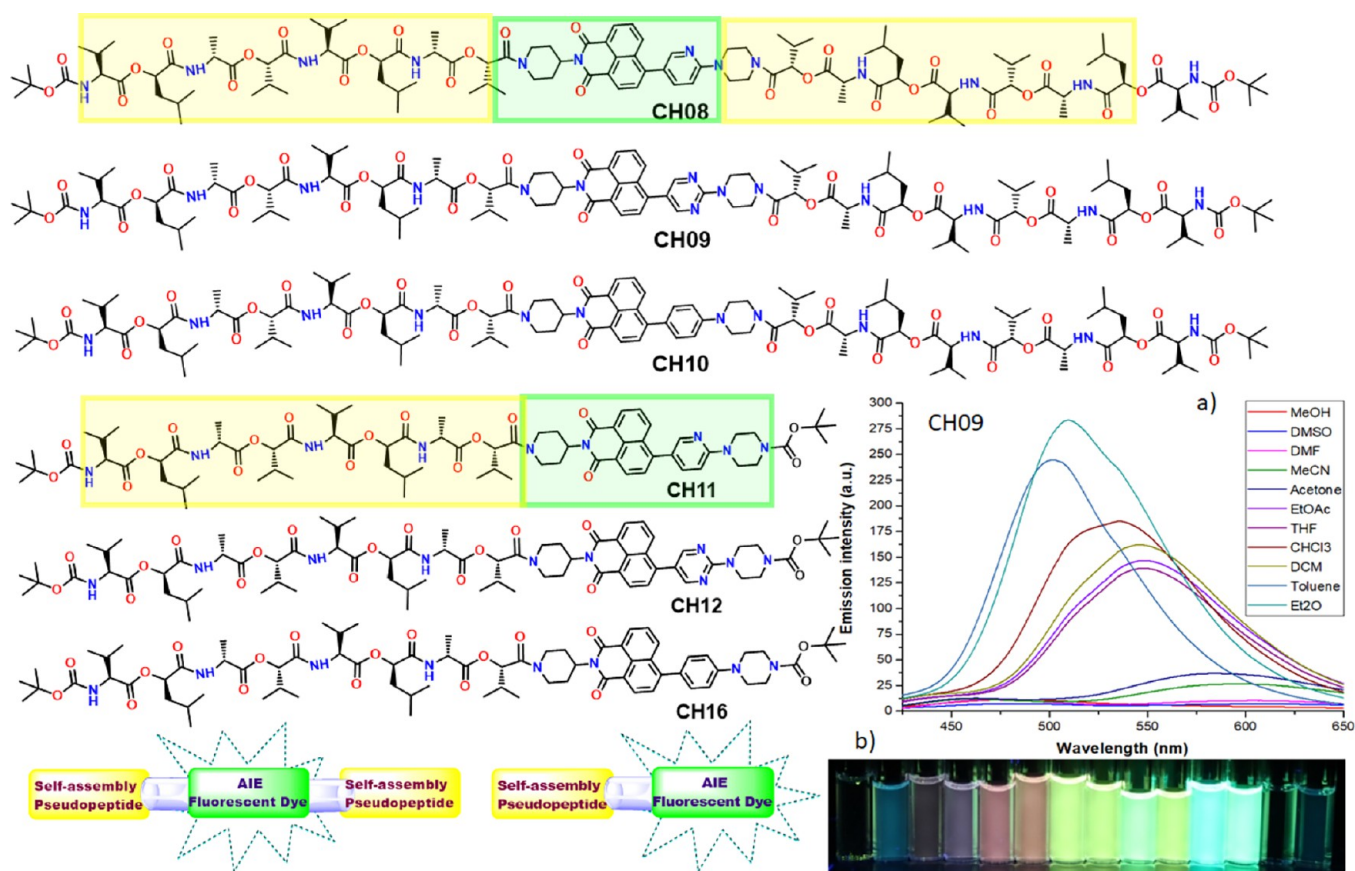


**Figure 1.** New hybrids of AIEgens and depsipeptide chains: (a) fluorescent emission of CH09 in solvents and (b) photography under UV light, from left to right, MeOH–Et<sub>2</sub>O.

their shelf life is very limited in living systems. In contrast, depsipeptides are nonribosomal peptide derivatives in which some amide groups have been replaced by ester groups,<sup>25</sup> which gives more flexibility to the depsipeptide structures and greater resistance to proteolysis by enzymes, but their self-assembly has been much less studied, so they constitute a rich source of new structural possibilities in the construction of nanomaterials. They are known to form nanofibers and  $\beta$ -sheet gels<sup>26,27</sup> or hydrogels,<sup>28</sup> but there are no previous studies on vesicle or nanoaggregate formation. Therefore, the combination of depsipeptides and AIEgens could provide a solution to the drawbacks posed by previous methodologies. Naphthalimides are known as AIEgens<sup>29</sup> and can form nanosheets<sup>30</sup> or metallogels<sup>31</sup> and are useful in super resolution,<sup>32</sup> making them suitable structures, in combination with depsipeptides, for the creation of vesicles based on supramolecular self-assembly and molecular recognition between structural components. These systems would be a great remedy to solving important current problems associated with the cellular transport of drugs or relevant physiological peptides, as well as nonwater-soluble coordination compounds in photodynamic therapy<sup>33</sup> or metal complexes for biomedical applications,<sup>34</sup> in addition to the nanoencapsulation of biocatalysts<sup>35</sup> or photocatalysts<sup>36</sup> in aqueous media. Taking this empty niche of research, we have carefully honed the creation of empty robust soft nanovesicles capable of accomplish all the required characteristics for active cell transport and nanoencapsulation with easy preparation and great versatility. This constitutes a radically new approach to the construction of cellular nanocarriers in which, by controlling the structural components of the

nanovesicles, we can switch from passive to active nanocarriers programmed in time, providing a solution to an important issue in nanomedicine and nanotechnology. In this way, we have previously shown that cyclic depsipeptides, that are K<sup>+</sup>-selective membrane ionophores, have implications for glucose-stimulated insulin secretion in  $\beta$ -cells and can be used as biomarkers in INS1E cells<sup>37</sup> and preimplantation factor, PIF, a naturally occurring peptide was useful for improving glucose-stimulated insulin secretion.<sup>38</sup> We have also developed new naphthalimides with electron-donating and electron-withdrawing groups in the structure, and amino-protective substituents in which variation of the substituents allowed the control of AIE characteristics, so the AIEgen fluorescence emission mechanism could be activated with optimal performance through structural modification.<sup>39,40</sup> We have recently discovered that some enzymes in insect saliva are useful for the degradation of polyethylene,<sup>41,42</sup> demonstrating that nanoencapsulation of catalysts has great potential. We realized that those achievements could be of interest for targeting nanostructures to specific cells or tissues.<sup>43–45</sup> Using structural designs from our previous experience, we developed novel organic nanostructures composed of aggregation-induced emission dyes linked to self-assembled depsipeptides, which together promoted supramolecular self-assembly into fluorescent nanovesicles. These nanovesicles were verified to be effective cellular biomarkers and nanocarriers. AFM and FESEM showed soft and hollow nanovesicles, obtained solely by self-assembly of the depsipeptide-AIEgen hybrid structures. We used these nanostructures to transport active peptides to cellular compartments acting simultaneously as biomarkers and

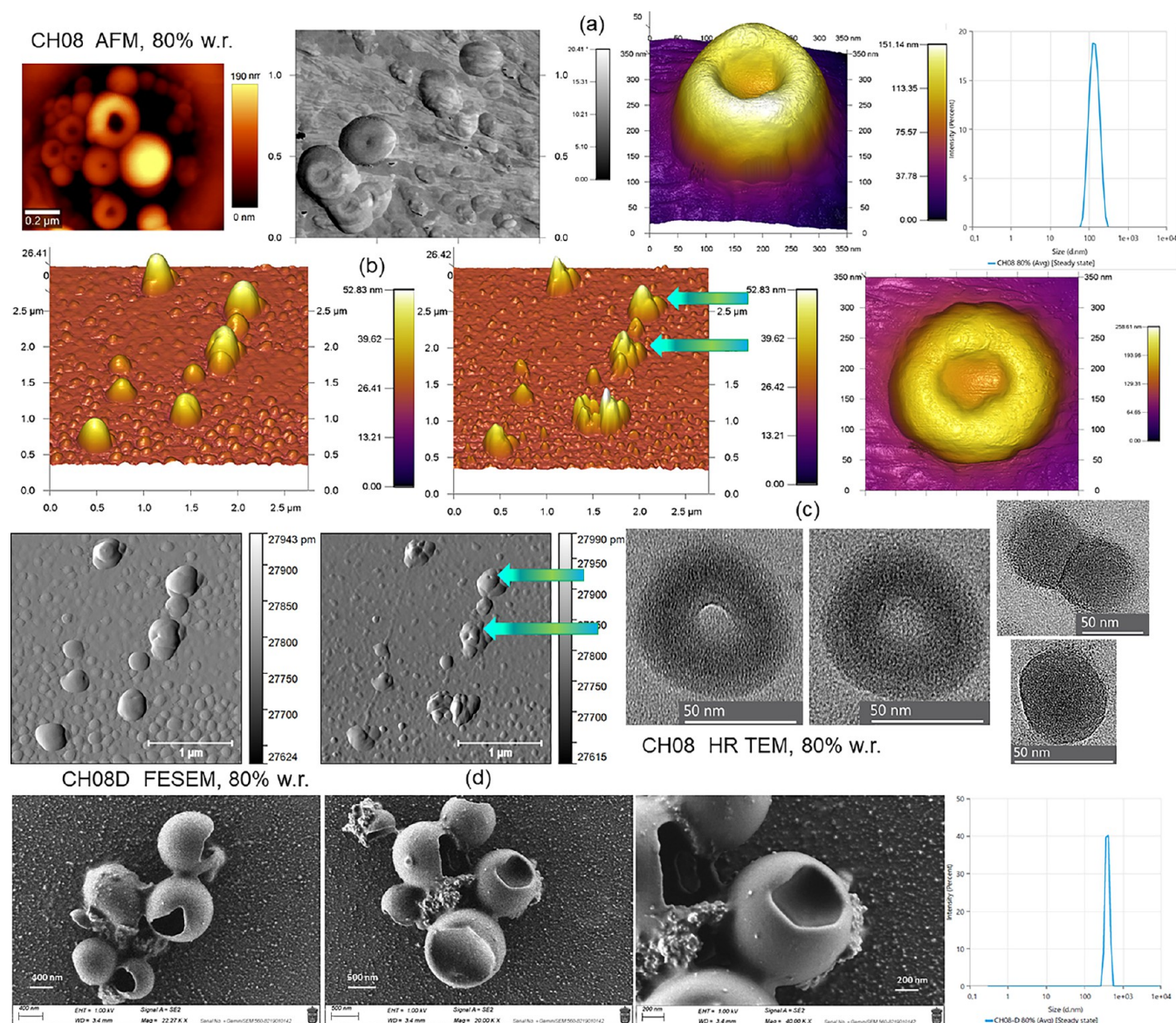


**Figure 2.** Nanoparticle imaging of a bifunctionalized NMI-bis-pseudopeptide CH08: (a) by low resolution AFM, high resolution AFM and DLS, (b) “Drilling a hole” by AFM typing on the nanovesicles of NMI-bis-pseudopeptide CH08; in addition, the vesicle at the center/lower part of the image was actually completely deformed, (c) by high resolution TEM of selected nanovesicles, (d) FESEM study of the N-Boc-protected de-Boc-CH08 (CH08-D) showing fractures on the surface of the hollow nanovesicles, DLS.

nanocarriers. As instance, PIF was successfully delivered via nanovesicles into cells of the human lung cancer cell line A549, were it could act as a very powerful nanocarrier of general application or as a time-scheduled active cytotoxic nanostructure for subsequent cell apoptosis. This fills an important gap in the development of new pharmaceuticals or nanocontainers for biocompatible processes. The results of the study are presented here.

## EXPERIMENTAL SECTION

Materials and methods are described in full in the [Supporting Information Section, pp. S4–S7](#), followed by the synthesis and complete characterization of all compounds used for the study, [pp. S8–S213](#).

## RESULTS AND DISCUSSION

**Preparation of Materials.** We have previously synthesized some fluorogenic probes for various types of analytes, by using Suzuki and Sonogashira reactions.<sup>37,39,40,46–52</sup> Between them, naphthalimides (NMIs) with protected amino groups<sup>39</sup> showed an increase in fluorescence in mixtures of organic solvents with water, an aggregation-induced emission effect (AIEgen) that disappeared when the structures contained unprotected amino groups. Taking advantage of the self-association of natural decapeptide chains by hydrogen bonds<sup>37</sup> and the self-assembly capacity of AIEgens,<sup>39,40</sup> we combined a short sequence of the natural decapeptide (eight units) and the AIEgen naphthalimides to obtain new AIEgen-decapeptide hybrids that were found to be highly fluorescent and solvatochromic ([Figure 1](#)) while maintaining the AIE-gen characteristics intact.

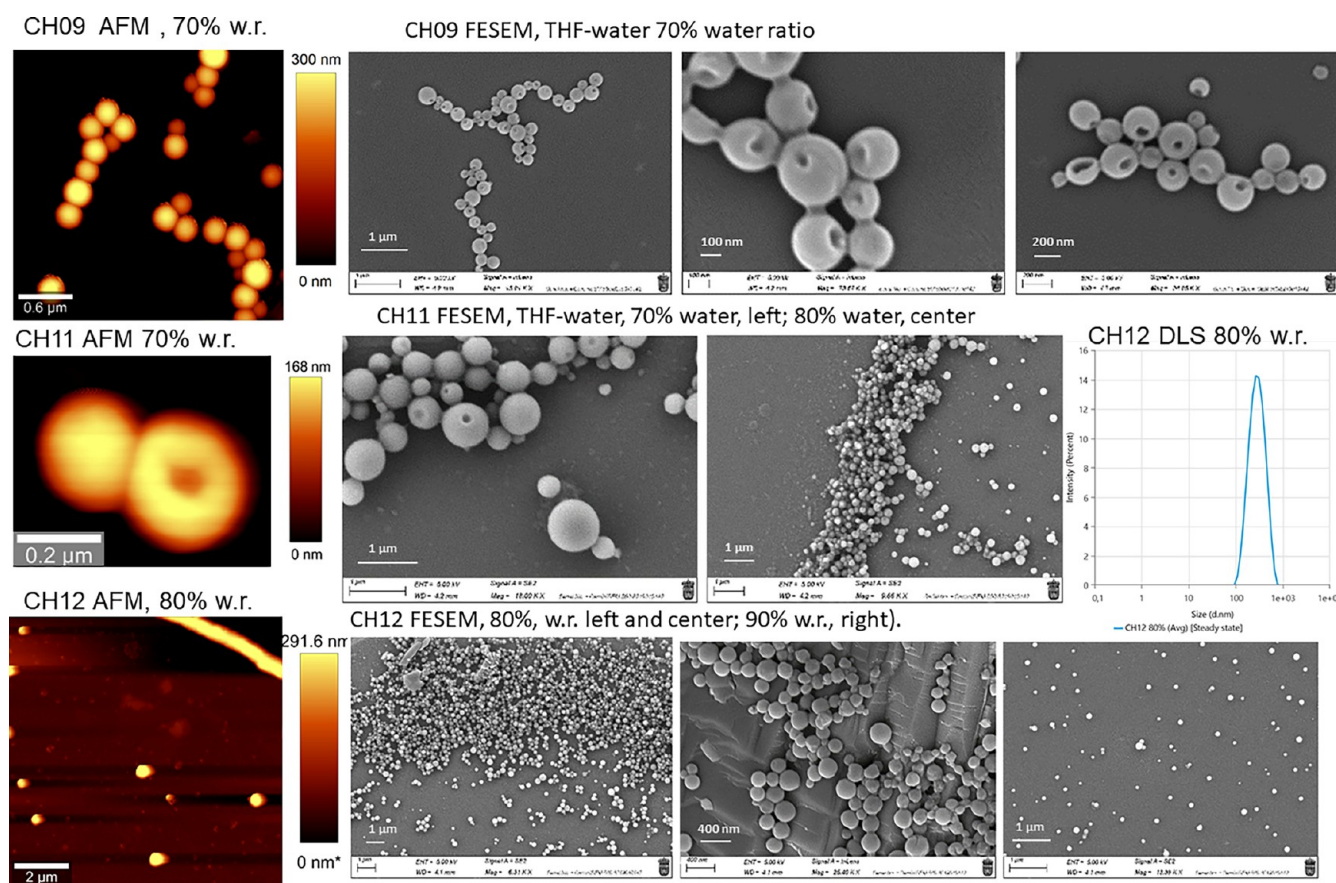


**Figure 3.** Images of CH09 nanoparticles, hollow vesicles observed by FESEM, CH09 (THF–water 70% water), images of CH11 nanoparticles, toroids, vesicles, observed by FESEM of CH11 (THF–water, 70% water, left; 80% water, center). Images of CH12 nanoparticles and distribution in DLS (THF–water, 80% water, left and center; 90% water, right).

For instance, the compound CH08 showed an increase in fluorescence as the amount of water in the solvent increased. Low-resolution AFM showed the formation of toroidal and spherical nanoparticles that in FESEM appeared as empty vesicles and well-formed spherical nanoparticles (Figure 2a), which was also confirmed by high-resolution AFM and by DLS measurements (Figure 2a). To solve the question of the hollow cavity of nanoparticles we decided to “drill a hole” in the nanovesicles by changing the typing mode in AFM, from which we could arrive to punctured vesicles from the intact ones (Figure 2b). Similar nanovesicles were also detected by high resolution TEM of CH08 by staining with uranyl acetate (Figure 2c). An additional FESEM study of an *N*-Boc-deprotected compound, de-Boc-CH08 (CH8-D) provided much clearer images of intact samples showing fractures on the surface of the hollow nanovesicles (Figure 2d) confirmed by DLS. In this way a clear difference could be found between an open nanovesicle and a “deflated” nanovesicle (Figure 2d).

Compound CH09 also showed an increase in fluorescence as the amount of water in the solvent increased. Low-resolution AFM showed the formation of spherical nanoparticles (Figure 3). The result was confirmed by FESEM (Figure 3). Of the single-branch depsipeptide-AIEgens, compound CH11 also showed an increase in fluorescence as the amount of water in the solvent increased. Low-resolution AFM showed toroidal and spherical nanoparticles (Figure 3). FESEM images of CH11, 70% water, confirmed the morphology of toroids and vesicles (Figure 3). The samples

deposited from 80% water showed by FESEM a homogeneous distribution of nanovesicles (Figure 3). Compound CH12 also showed an increase in fluorescence in relation to the amount of water in the solvent. Low-resolution AFM showed formation of spherical, fluorescent nanoparticles in fluorescence microscopy (Figure 3). FESEM of CH12 samples, deposited from THF–water, 80% and 90% water, confirmed the morphology of the vesicles, showing in both cases a homogeneous distribution of nanovesicles, also confirmed by DLS (Figure 3).

**Cell Transport.** To develop the possibilities of the described nanovesicles as potential drug carriers, we first tested a model compound, *N*-Boc-deprotected-CH11 (CH11-D), first we checked the integrity of AIEgen characteristics in DMSO/water by AFM (see Supporting Information, p. 96) and then we studied colocalization in A549 cells (Figure 4). By confocal laser scanning microscopy (CLSM) we found that the nanovesicles showed positive colocalization with endoplasmic reticulum (ER) (Figure 4) stained with ER Tracer Blue (AAT Bioquest). The study by stimulated emission depletion (STED) super-resolution microscopy showed that the size of the nanovesicles matched that found by AFM and FESEM, so the nanovesicles were integrated into living cells (Figure 4). Next, we studied the transport of active peptides to cellular compartments by using nanovesicles to transport an active peptide, preimplantation factor (PIF), modified for bioconjugation (Figure 4). We checked the integrity of AIEgen in DMSO/water (99.5%) of CH28 and CH48 by AFM and FESEM, and studied colocalization in A549 cells (Figure 4).

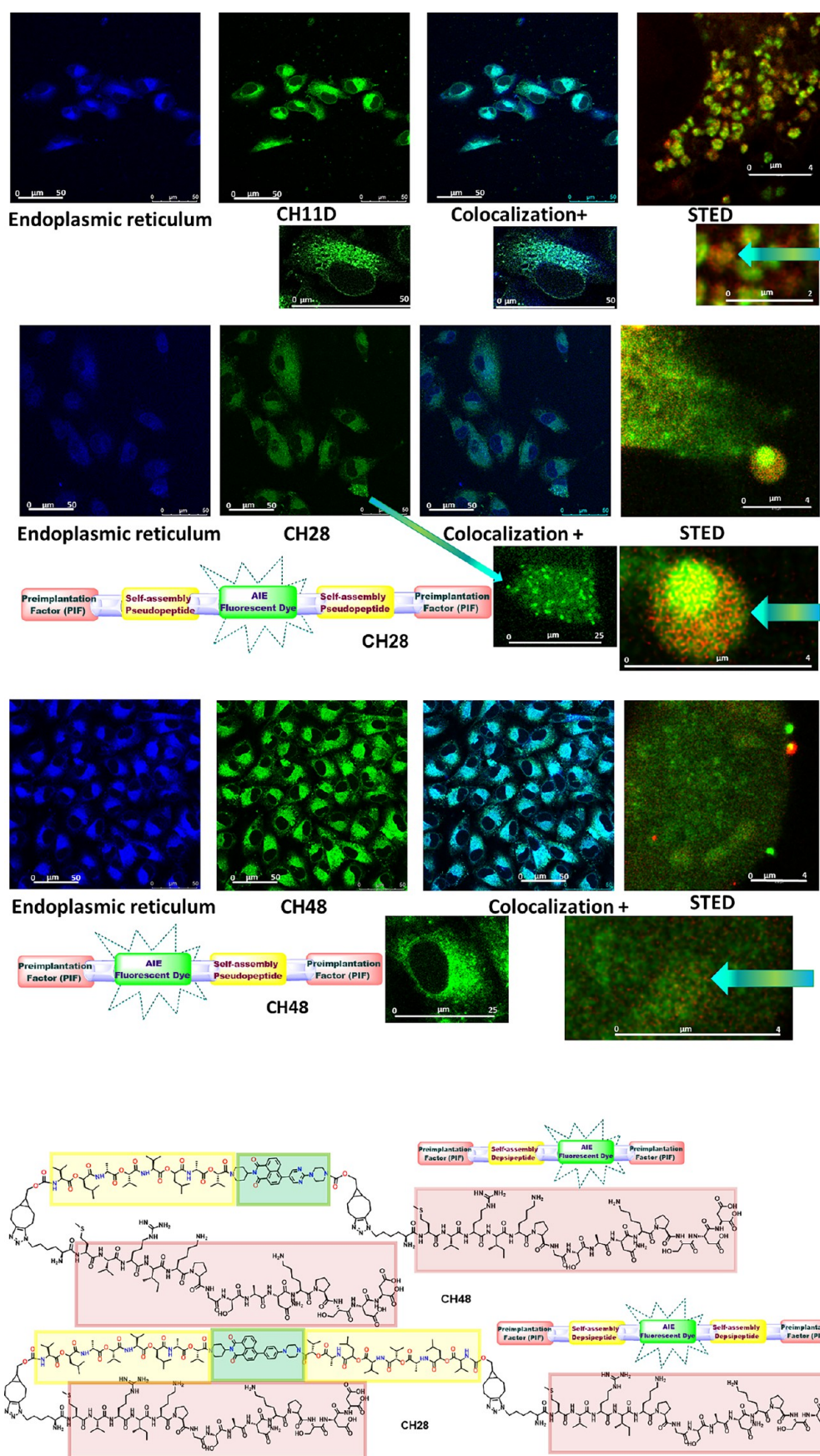
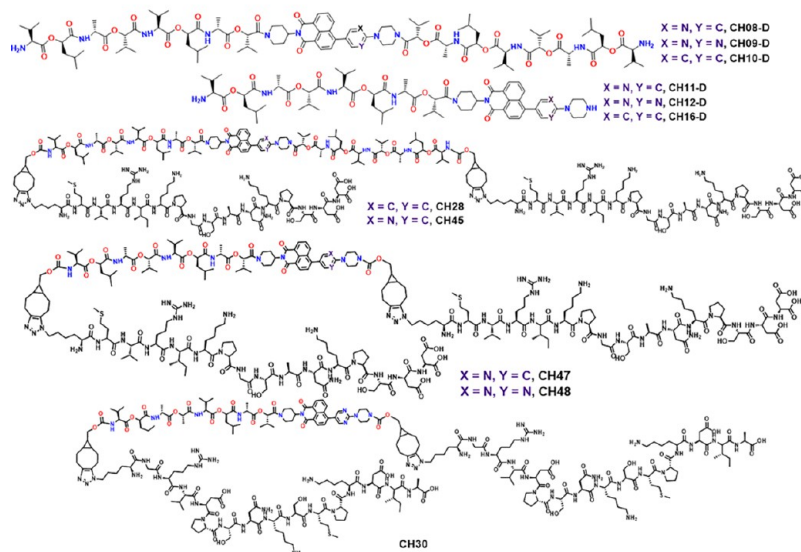


**Figure 4.** Confocal laser scanning microscopy (CLSM) and STED super-resolution microscopy of CH11D, CH48, and CH28. Inset: Structures of new AIEgen-depsipeptide-PIF hybrids for cellular delivery.

Table 1. IC<sub>50</sub> Values ( $\mu\text{M}$ ) after 24 or 72 h of Treatment, Mean  $\pm$  SD from 3 or More Independent Experiments<sup>a</sup>

	A549 24h	A549 72h	A2780 24h	A2780cis 24h
CH11	>100	-	-	-
CH08-D	>100	>100	>100	>100
CH09-D	>100	>100	>100	>100
CH10-D	>100	>100	>100	>100
CH11-D	6.1 $\pm$ 0.5	3.6 $\pm$ 0.7	4.4 $\pm$ 0.4	4.0 $\pm$ 0.3
CH12-D	3.8 $\pm$ 0.5	2.6 $\pm$ 0.1	2.4 $\pm$ 0.1	1.6 $\pm$ 0.1
CH16-D	12.3 $\pm$ 0.8	6.05 $\pm$ 0.2	4.6 $\pm$ 0.6	4.1 $\pm$ 0.3
CH30	>100	43.6 $\pm$ 2.3	>100	>100
CH28	>100	>100	>100	>100
CH45	>100	>100	>100	>100
CH47	84.5 $\pm$ 9.1	48.5 $\pm$ 2.1	13.1 $\pm$ 0.6	45.5 $\pm$ 3.4
CH48	54.8 $\pm$ 2.9	22.7 $\pm$ 2.6	20.9 $\pm$ 1.2	29.5 $\pm$ 0.8
CDDP	46.3 $\pm$ 3.9	4.6 $\pm$ 0.3	8.0 $\pm$ 0.9	29.8 $\pm$ 2.7

<sup>a</sup>CDDP is included as positive control.



By CLSM (LEICA TCS SP8 STED 3X) we found that the nanovesicles showed positive colocalization with the endoplasmic reticulum (Figure 4). The STED study showed that the size was similar by the STED, AFM and FESEM techniques, demonstrating that the nanovesicles were integrated into living cells while maintaining the size of their nanostructure (Figure 4). For CLSM 50  $\mu\text{M}$ ,  $\lambda_{\text{exc}} = 470$  nm and  $\lambda_{\text{em}} = 670$  nm. Colocalization coefficients were calculated with ImageJ. To evaluate the spatial overlap between the two signals, Pearson's correlation coefficient and Manders' colocalization coefficients (M1 and M2) were calculated. For CH11-D, Pearson's correlation coefficient (Rr, no threshold): 0.81, showing a strong positive correlation between the intensity distributions of CH11D and the ER probe; Manders' coefficients: M1 (CH11D overlapping ER probe): 0.890, M2 (ER probe overlapping CH11D): 0.616; these values indicated that 89.0% of CH11D signal overlaps with the ER probe, and 61.6% of the ER probe signal overlaps with CH11D across the

entire field of view. For CH28, the analysis yielded the following results: Pearson's correlation coefficient (Rr, no threshold): 0.63, indicating a moderate positive correlation between the intensity distributions of CH28 and the ER probe. Manders' coefficients: M1 (CH28 overlapping ER probe): 0.692, M2 (ER probe overlapping CH28): 0.642, these values indicated that 69.2% of CH28 signal overlaps with the ER probe, and 64.2% of the ER probe signal overlaps with CH28. For CH48, the analysis yielded the following results: Pearson's correlation coefficient (Rr, no threshold): 0.68, indicating a moderate positive correlation between CH48 and the ER probe. Manders' coefficients: M1 (CH48 overlapping ER probe): 0.667, M2 (ER probe overlapping CH48): 0.586, this indicated that 66.7% of the CH48 signal resided in regions where the ER-specific probe was present and that 58.6% of the ER probe signal overlapped with CH48.

**Antiproliferative Activity.** Table 1 shows the IC<sub>50</sub> values ( $\mu\text{M}$ ) after 24 h or 72 h of treatment, mean  $\pm$  SD from at least

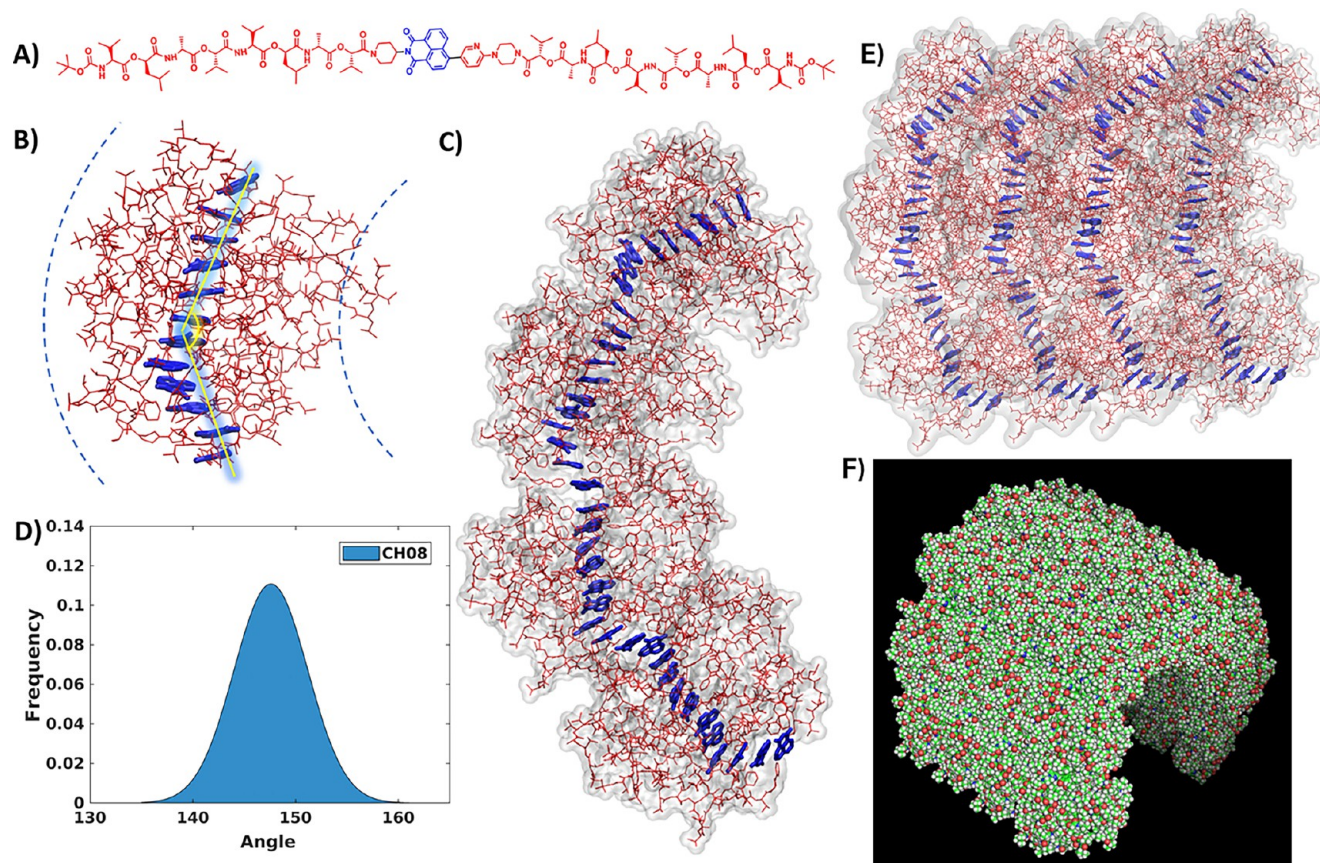


**Figure 5.** (A) Computational atomistic model of CH08. The aromatic naphthalimide core is shown in blue, while the depsipeptide chains are shown in red. (B) Representative structure as extracted from a molecular dynamics trajectory of 12 stacked CH08 monomers showing the tilt angle measured between the central monomer and the top and bottom monomers. (C) The extended model was obtained from replicating our simulated ones. (D) Tilt angle distribution during the MD simulation. (E) A model of the interaction of four stacked CH08 sets of molecules. (F) The CPK model of the curvature of the four stacked CH08 sets of molecules from (E).

2 independent experiments, cisplatin (*cis*-[Pt(NH<sub>3</sub>)<sub>2</sub>Cl<sub>2</sub>], *cis*-diamminedichloroplatinum(II), CDDP) is included as positive control. The study was performed by using three cell types, lung tumor cells A549, human ovarian carcinoma cell line A2780 (cisplatin-sensitive) and A2780cis (cisplatin-resistant), confirming the general behavior of the different types of nanovesicles; thus, CH08-D, CH09-D and CH10-D were biocompatible, noncytotoxic either at 24 or 72 h; CH11-D, CH12-D and CH16-D were cytotoxic at 24 h, IC<sub>50</sub> 2–12 μM, CH28 (CH10-D+2PIF) and CH45 (CH08-D + 2PIF) were biocompatible and noncytotoxic; CH47 (CH11-D + 2PIF) and CH48 (CH12-D + 2PIF) in turn, showed low cytotoxicity at 24 h, IC<sub>50</sub> 55–85 μM, and an appreciable increase of cytotoxicity after 72 h, IC<sub>50</sub> 23–49 μM on A549 cells, and an enhanced cytotoxicity at 24 h, IC<sub>50</sub> 13–46 μM on A2780/A2780cis cells. Naphthaleneimides without depsipeptide moiety were not suitable for cell studies because of their low solubility in the cell media, that leads to precipitation and easy atmospheric oxidation. According to all the collected results, the presence of the second depsipeptide significantly decreased the cytotoxicity of the derivatives. The same trend was observed when PIF units were added, therefore the type of structure strongly influenced antiproliferative activity of the compounds. This finding opened the possibility of modulating the action of nanovesicles for transporting sensitive drugs such as PIF, which is a physiological peptide, easily degraded in biological environments, by using a type of noncytotoxic

vesicle, or for acting as a Trojan horse by carrying a cytotoxic cargo with a physiologically innocent outer envelope that, after degradation, delivers its cargo promoting cell apoptosis. This effect was more dramatic by using a derivative having a scrambled PIF, CH30, which was noncytotoxic at 24 h, proving that the physiological action of the natural PIF is necessary to exert activity in cells.

In order to obtain atomistic details of the nanovesicles structure we have built a model of interacting CH08 monomers and we have run μs-long molecular dynamics (MD) simulations. This technique, by exploring the dynamical properties of a molecular system, can furnish important insight into the structural features and self-assembly of supramolecular systems.<sup>53</sup> Interestingly, our MD simulations show that the aromatic naphthalimide core performs stable  $\pi$ - $\pi$  stacking interactions and overall adopts a peculiar bending toward a vesicular structure (Figure 5b,d). On average, this tilt of about 147° shows that the simulated model can account for the curvature of the nanovesicle wall. This becomes particularly clear if we extend our model by replicating the stacking interactions performed by the aromatic core (Figure 5d). From the calculations, an estimation of the thickness of the CH08 associated ensemble would be about 5 nm; from Figure 2, bottom row, the calculated thickness of the nanovesicle wall is apparently about 20 nm, therefore the nanovesicle wall appears to be composed by an average thickness of four curved

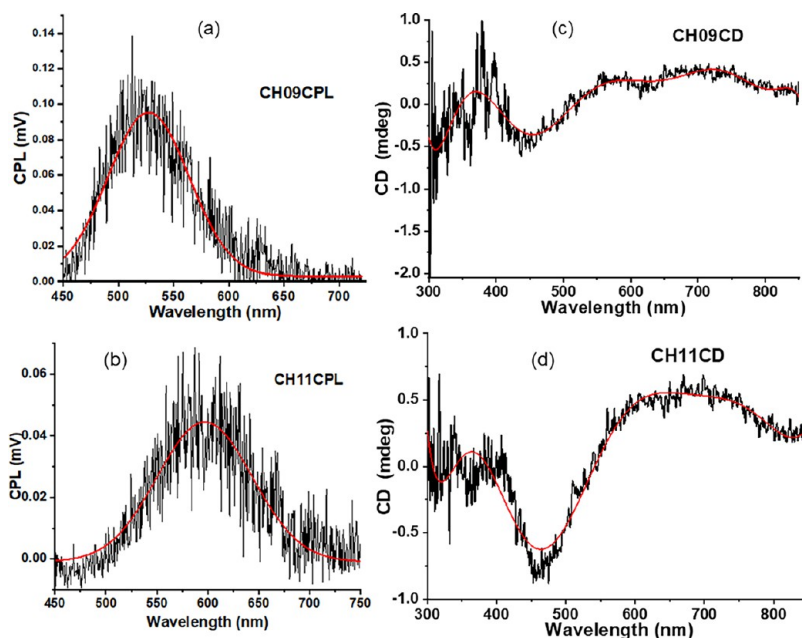


**Figure 6.** Circularly polarized luminescence spectra showing the relative circularly polarized luminescence from CH09 (a) and CH11 (b) (10 avg. spectra,  $L(x) = 390$  nm and  $t(acq.) = 1$  ms/nm). The corresponding circular dichroism spectra of CH09 (c) and CH11 (d).

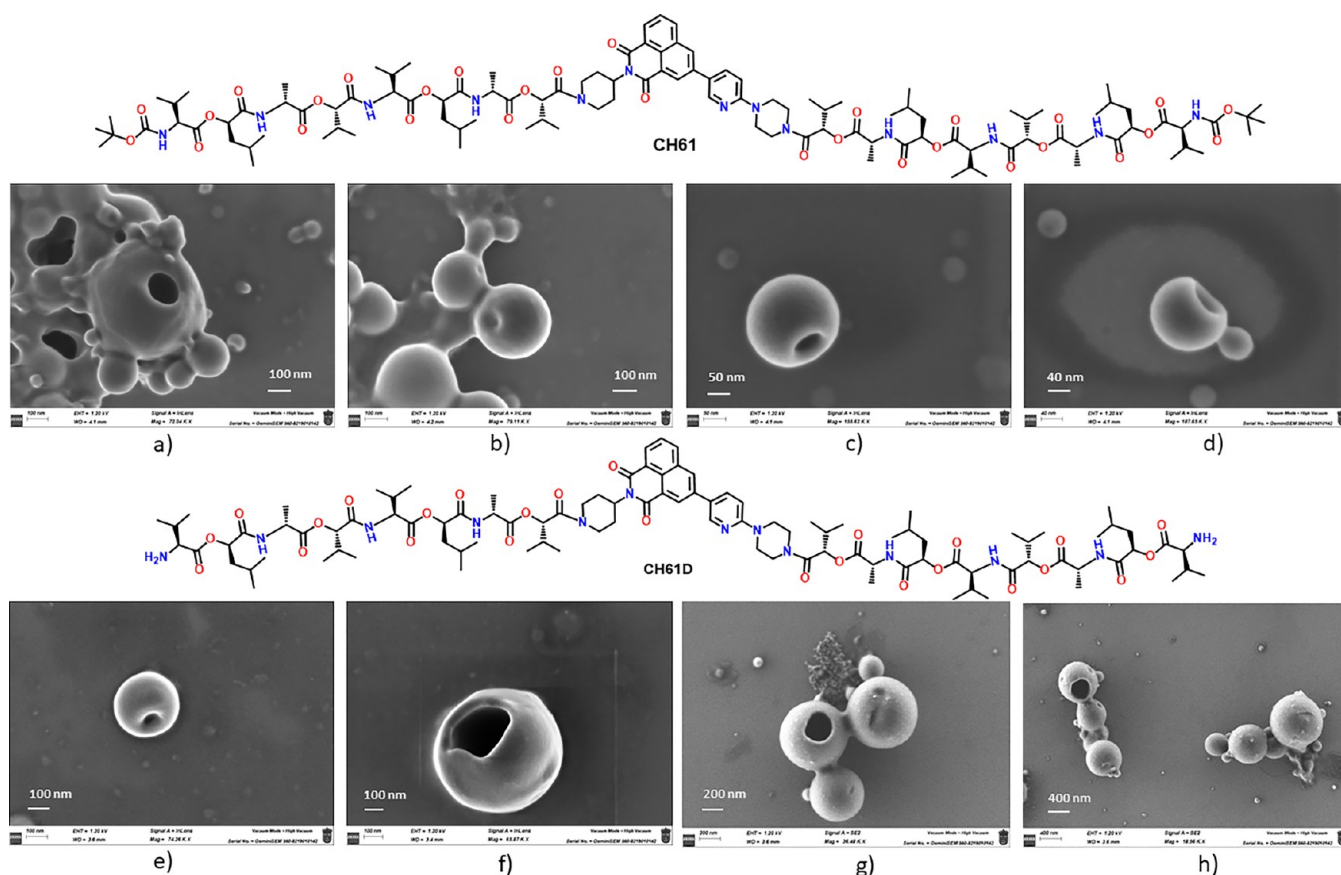


**Figure 7.** Images of CH61/CH61D nanoparticles, hollow vesicles observed by FESEM: CH61 (THF–water, 80% water, a,b; 90% water, c,d); CH61D (THF–water, 70% water, e; 80% water, f; 90% water, g,h).

associated entities as calculated in Figure 5c and modeled in Figure 5e,f.

Another important issue in the mechanism of formation of such nanostructures is the characteristics that rigidity confers to the ensemble. Stacking of simple chiral groups and the core

dye produces chiral nanoentities that give macroscopic responses as a circularly polarized luminescence (CPL) and circular dichroism (CD) signals, which are only seen when the nanostructure formation is completed (Figure 6).

From those studies we have mastered the control of conditions for the formation of nanovesicles, cell permeability and cytotoxicity. The proof of concept developed permitted prediction of nanostructures with accuracy. For example, we have modified the geometry of the core dye, added depsiptide chains, and obtained nanovesicles alike (Figure 7).

## CONCLUSION

We have described the proof of concept of a new methodology to produce robust hollow nanovesicles stable in water or mixtures of water and organic solvents. The bottom-up produced nanovesicles are formed by self-assembly of depsiptide chains of natural origin combined with new aggregation induced emission luminogens that function as constitutional vesicle-forming moieties and fluorescent indicators of the structure of the nanovesicle. The newly formed nanovesicles are robust enough to be used to carry large molecules such as physiological peptides without losing their structural characteristics, therefore acting as programmable nanocarrier systems within living cells as a radically new approach to active transport and nanoencapsulation. Those nanovesicles, localized in the endoplasmic reticulum, have shown perfect biocompatibility when having a dye and two depsiptides, or high cytotoxicity, which is modulable by the presence of physiological peptides such as PIF, which activities much higher than cisplatin for members having only one depsiptide moiety, in all tested cancer cell lines. This opens the door to its use as a Trojan horse for cancer cell fighting research.

## ASSOCIATED CONTENT

### Supporting Information

The Supporting Information is available free of charge at <https://pubs.acs.org/doi/10.1021/acsami.4c19123>.

Complete characterization for all compounds, additional experimental details, and materials and methods (PDF)

## AUTHOR INFORMATION

### Corresponding Authors

**Tomás Torroba** – Department of Chemistry, Faculty of Science, University of Burgos, Burgos 09001, Spain; [orcid.org/0000-0002-5018-4173](https://orcid.org/0000-0002-5018-4173); Email: [ttorroba@ubu.es](mailto:ttorroba@ubu.es)

**Natalia Busto** – Department of Health Science, Faculty of Health Science, University of Burgos, Burgos 09001, Spain; Email: [nbusto@ubu.es](mailto:nbusto@ubu.es)

### Authors

**Carla Hernando-Muñoz** – Department of Chemistry, Faculty of Science, University of Burgos, Burgos 09001, Spain

**Andrea Revilla-Cuesta** – Department of Chemistry, Faculty of Science, University of Burgos, Burgos 09001, Spain

**Irene Abajo-Cuadrado** – Department of Chemistry, Faculty of Science, University of Burgos, Burgos 09001, Spain

**Camilla Andreini** – Department of Chemistry, Faculty of Science, University of Burgos, Burgos 09001, Spain

**Darío Fernández** – Department of Health Science, Faculty of Health Science, University of Burgos, Burgos 09001, Spain; [orcid.org/0000-0002-9763-7328](https://orcid.org/0000-0002-9763-7328)

**German Perdomo** – Instituto de Biomedicina y Genética Molecular (IBGM), Consejo Superior de Investigaciones

Científicas (CSIC) y Universidad de Valladolid, Valladolid 47003, Spain

**Gerardo Acosta** – Instituto de Química Avanzada de Cataluña (IQAC-CSIC), Barcelona 08034, Spain

**Miriam Royo** – Instituto de Química Avanzada de Cataluña (IQAC-CSIC), Barcelona 08034, Spain; [orcid.org/0000-0001-5292-0819](https://orcid.org/0000-0001-5292-0819)

**Javier Gutierrez Reguera** – LTI, I+D Uvainnova-Campus Miguel Delibes, University of Valladolid, Valladolid 47011, Spain; [orcid.org/0000-0001-9163-0072](https://orcid.org/0000-0001-9163-0072)

**Angelo Spinello** – STEBICEF Department, Università degli Studi di Palermo, Palermo 90128 Sicilia, Italy

**Giampaolo Barone** – STEBICEF Department, Università degli Studi di Palermo, Palermo 90128 Sicilia, Italy; [orcid.org/0000-0001-8773-2359](https://orcid.org/0000-0001-8773-2359)

**Dominic Black** – Department of Chemistry, Durham University, Durham DH1 3LE, U.K.

**Robert Pal** – Department of Chemistry, Durham University, Durham DH1 3LE, U.K.

Complete contact information is available at: <https://pubs.acs.org/doi/10.1021/acsami.4c19123>

## Author Contributions

The manuscript was written through contributions of all authors. All authors have given approval to the final version of the manuscript. T.T.: supervised the work and wrote the manuscript with the contributions of all authors. N.B.: supervised the biological work, carried out part of the biological research, and wrote the biological section of the manuscript. C.H.-M.: carried out laboratory research, synthesis and spectroscopic characterization of compounds, and wrote a large section of the Supporting Information of the manuscript. A.R.-C.: carried out laboratory research, synthesis and characterization of the AIE-gen dyes. I.A.-C.: carried out the fluorescent characterization of compounds, fluorescent tests, and wrote the fluorescence-specific section of the Supporting Information of the manuscript. C.A.: carried out part of the biological research and wrote a preliminary report on the biological results. D.F.: contributed to the confocal microscopy experiments and colocalization studies. G.P.: supervised the work with PIF. G.A.: synthesized the modified PIF for bioconjugation. M.R.: designed and supervised the work with the modified PIF for bioconjugation. J.G.R.: performed the high-resolution AFM work and the DLS studies. A.S.: performed the calculations on the aggregation structures. G.B.: designed and supervised the calculations on the aggregation structures and wrote the conclusions from the calculations. D.B.: performed the CPL measurements. R.P.: designed and supervised the CPL measurements.

## Notes

The authors declare no competing financial interest.

## ACKNOWLEDGMENTS

This research was funded by the *Ministerio de Ciencia, Innovación y Universidades* of Spain (Grants PDC2022–133955-I00 and PID2022–142318NB-I00). C.H.-M. thanks the *Secretaría General de Universidades* of Spain for an FPU21/01473 Grant. The authors thank Dr. José García-Calvo, from the Organic Chemistry Dept., Science Faculty, UAM, Madrid, for assistance with DC spectroscopy and Dr. Manuel Avella, from IMDEA Materials Institute, Tecnogetafe, Madrid, for assistance with TEM.

## REFERENCES

- (1) Zhao, J.; Chen, O.; He, J.; Zou, S. Metal and semiconductor nanocrystals. *Front. Chem.* **2019**, *7*, 310.
- (2) Ma, J.; Wang, H.; Li, D. Recent progress of chiral perovskites: materials synthesis and properties. *Adv. Mater.* **2021**, *33*, 2008785.
- (3) Pokrajac, L.; Abbas, A.; Chrzanoski, W.; Dias, G. M.; Eggleton, B. J.; Maguire, S.; Maine, E.; Malloy, T.; Nathwani, J.; Nazar, L.; et al. Nanotechnology for a sustainable future: addressing global challenges with the international network4sustainable nanotechnology. *ACS Nano* **2021**, *15* (12), 18608–18623.
- (4) Pattipeiluhu, R.; Arias-Alpizar, G.; Basha, G.; Chan, K. Y. T.; Bussmann, J.; Sharp, T. H.; Moradi, M.; Sommerdijk, N.; Harris, E. N.; Cullis, P. R.; Kros, A.; Witzigmann, D.; Campbell, F. Anionic lipid nanoparticles preferentially deliver mRNA to the hepatic reticuloendothelial system. *Adv. Mater.* **2022**, *34*, 2201095.
- (5) Das, R.; Kanjilal, P.; Medeiros, J.; Thayumanavan, S. What's next after lipid nanoparticles? A perspective on enablers of nucleic acid therapeutics. *Bioconjugate Chem.* **2022**, *23*, 1996–2007.
- (6) Wang, Z.; Sun, C.; Wang, R. Macrocyclic-surfaced polymer nanocapsules: an emerging paradigm for biomedical applications. *Bioconjugate Chem.* **2022**, *33*, 2254–2261.
- (7) Mitchell, M. J.; Billingsley, M. M.; Haley, R. M.; Wechsler, M. E.; Peppas, N. A.; Langer, R. Engineering precision nanoparticles for drug delivery. *Nat. Rev. Drug Discovery* **2020**, *21*, 101–124.
- (8) Huo, Y.; Hu, J.; Yin, Y.; Liu, P.; Cai, K.; Ji, W. Self-assembling peptide-based functional biomaterials. *ChemBiochem* **2023**, *24*, No. e202202.
- (9) Qiu, R.; Sasselli, I. R.; Álvarez, Z.; Sai, H.; Ji, W.; Palmer, L. C.; Stupp, S. I. Supramolecular copolymers of peptides and lipidated peptides and their therapeutic potential. *J. Am. Chem. Soc.* **2022**, *144*, 5562–5574.
- (10) Haridas, V. Tailoring of peptide vesicles: A bottom-up chemical approach. *Acc. Chem. Res.* **2021**, *54*, 1934–1949.
- (11) Levin, A.; Hakala, T. A.; Schnaider, L.; Bernardes, G. J. L.; Gazit, E.; Knowles, T. P. J. Biomimetic peptide self-assembly for functional materials. *Nat. Rev. Chem.* **2020**, *4*, 615–634.
- (12) Khan, I.; Hossain, I.; Hossain, K.; Rubel, H. K.; Hossain, K. M.; Mahfuz, A. M. U. B.; Anik, M. I. Recent progress in nanostructured smart drug delivery systems for cancer therapy: A review. *ACS Appl. Bio Mater.* **2022**, *5* (3), 971–1012.
- (13) Sheehan, F.; Sementa, D.; Jain, A.; Kumar, M.; Tayarani-Najjaran, M.; Kroiss, D.; Ulijndoi, R. V. Peptide-based supramolecular systems chemistry. *Chem. Rev.* **2021**, *121* (22), 13869–13914.
- (14) Chatterjee, A.; Reja, A.; Pal, S.; Das, D. Systems chemistry of peptide-assemblies for biochemical transformations. *Chem. Soc. Rev.* **2022**, *51*, 3047–3070.
- (15) Song, Y.; Li, M.; Song, N.; Liu, X.; Wu, G.; Zhou, H.; Long, J.; Shi, L.; Yu, Z. Self-amplifying assembly of peptides in macrophages for enhanced inflammatory treatment. *J. Am. Chem. Soc.* **2022**, *144*, 6907–6917.
- (16) Manzari, M. T.; Shamay, Y.; Kiguchi, H.; Rosen, N.; Scaltriti, M.; Heller, D. A. Targeted drug delivery strategies for precision medicines. *Nat. Rev. Mater.* **2021**, *6*, 351–370.
- (17) Mei, J.; Leung, N. L. C.; Kwok, R. T. K.; Lam, J. W. Y.; Tang, B. Z. Aggregation-induced emission: together we shine, united we soar! *Chem. Rev.* **2015**, *115*, 11718–11940.
- (18) Zhao, Z.; He, W.; Tang, B. Z. Aggregate materials beyond AIEgens. *Acc. Mater. Res.* **2021**, *2*, 1251–1260.
- (19) Xiao, P.; Xie, W.; Zhang, J.; Wu, Q.; Shen, Z.; Guo, C.; Wu, Y.; Wang, F.; Tang, B. Z.; Wang, D. De novo design of reversibly pH-switchable NIR-II aggregation-induced emission luminogens for efficient phototherapeutics of patient-derived tumor xenografts. *J. Am. Chem. Soc.* **2023**, *145*, 334–344.
- (20) Li, W.; Schierle, G. S. K.; Lei, B.; Liu, Y.; Kaminski, C. F. Fluorescent nanoparticles for super-resolution imaging. *Chem. Rev.* **2022**, *122* (15), 12495–12543.
- (21) Sun, F.; Zhao, W.; Shen, H.; Fan, N.; Zhang, J.; Liu, Q.; Xu, C.; Luo, J.; Zhao, M.; Chen, Y.; Lam, K. W. K.; Yang, X.; Kwok, R. T. K.; Lam, J. W. Y.; Sun, J.; Zhang, H.; Tang, B. Z. Design of Smart Aggregates: toward rapid clinical diagnosis of hyperlipidemia in human blood. *Adv. Mater.* **2022**, *34*, 220767.
- (22) Liu, Y.; Teng, L.; Yin, B.; Meng, H.; Yin, X.; Huan, S.; Song, G.; Zhang, X. B. Chemical design of activatable photoacoustic probes for precise biomedical applications. *Chem. Rev.* **2022**, *122*, 6850–6918.
- (23) Yang, J.; Yu, X.; Song, J. I.; Song, Q.; Hall, S. C. L.; Yu, G.; Perrier, S. Aggregation-induced emission featured supramolecular tubosomes for imaging-guided drug delivery. *Angew. Chem., Int. Ed.* **2022**, *61*, No. e202115208.
- (24) Marciano, Y.; Solar, V. D.; Nayeem, N.; Dave, D.; Son, J.; Contel, M.; Ulijn, R. V. Encapsulation of gold-based anticancer agents in protease-degradable peptide nanofilaments enhances their potency. *J. Am. Chem. Soc.* **2023**, *145* (1), 234–246.
- (25) Spinck, M.; Piedrafita, C.; Robertson, W. E.; Elliott, T. S.; Cervettini, D.; Torre, D.; Chin, J. W. Genetically programmed cell-based synthesis of non-natural peptide and depsipeptide macrocycles. *Nat. Chem.* **2023**, *15* (1), 61–69.
- (26) Tian, Y. F.; Hudalla, G. A.; Hana, H.; Collier, J. H. Controllably degradable  $\beta$ -sheet nanofibers and gels from self-assembling depsipeptides. *Biomater. Sci.* **2013**, *1*, 1037–1045.
- (27) Nguyen, M. M.; Eckesa, K. M.; Suggs, L. J. Charge and sequence effects on the self-assembly and subsequent hydrogelation of Fmoc-depsipeptides. *Soft Matter* **2014**, *10* (15), 2693–2702.
- (28) Eckes, K. M.; Baek, K.; Suggs, L. J. Design and evaluation of short self-assembling depsipeptides as bioactive and biodegradable hydrogels. *ACS Omega* **2018**, *3*, 1635–1644.
- (29) Gopikrishna, P.; Meher, N.; Iyer, P. K. Functional 1,8-naphthalimide AIE/AIEEgens: recent advances and prospects. *ACS Appl. Mater. Interfaces* **2018**, *10*, 12081–12111.
- (30) Lin, H.; Wang, J.; Zhao, J.; Zhuang, Y.; Liu, B.; Zhu, Y.; Jia, H.; Wu, K.; Shen, J.; Fu, X.; Zhang, X.; Long, J. Molecular dipole-induced photoredox catalysis for hydrogen evolution over self-assembled naphthalimide nanoribbons. *Angew. Chem. Int. Ed.* **2022**, *61*, No. e202117645.
- (31) Lovitt, J. I.; Gorai, T.; Cappello, E.; Delente, J. M.; Barwich, S. T.; Möbius, M. E.; Gunnlaugsson, T.; Hawes, C. S. Supramolecular aggregation properties of 4-(1-morpholino)-1,8-naphthalimide based fluorescent materials. *Mater. Chem. Front.* **2021**, *5*, 3458–3469.
- (32) Qiao, Q.; Liu, W.; Zhang, Y.; Chen, J.; Wang, G.; Tao, Y.; Miao, L.; Jiang, W.; An, K.; Xu, Z. In situ real-time nanoscale resolution of structural evolution and dynamics of fluorescent self-assemblies by super-resolution imaging. *Angew. Chem., Int. Ed.* **2022**, *61*, No. e202208678.
- (33) Kuang, S.; Wei, F.; Karges, J.; Ke, L.; Xiong, K.; Liao, X.; Gasser, G.; Ji, H.; Chao, H. Photodecaging of a mitochondria-localized iridium(III) endoperoxide complex for two-photon photoactivated therapy under hypoxia. *J. Am. Chem. Soc.* **2022**, *144* (9), 4091–4101.
- (34) Amarsy, I.; Papot, S.; Gasserdoi, G. Stimuli-responsive metal complexes for biomedical applications. *Angew. Chem., Int. Ed.* **2022**, *61* (40), No. e202205900.
- (35) Sousa-Castillo, A.; Mariño-López, A.; Puértolas, B.; Correa-Duarte, M. A. Nanostructured heterogeneous catalysts for bio-orthogonal reactions. *Angew. Chem., Int. Ed.* **2023**, *62*, No. e202215427.
- (36) Zhang, N.; Trépout, S.; Chen, H.; Li, M. H. AIE polymer micelle/vesicle photocatalysts combined with native enzymes for aerobic photobiocatalysis. *J. Am. Chem. Soc.* **2023**, *145*, 288–299.
- (37) García-Calvo, J.; Torroba, T.; Brañas-Fresnillo, V.; Perdomo, G.; Cózar-Castellano, I.; Li, Y.-H.; Legrand, Y.-M.; Barboiu, M. Manipulation of transmembrane transport by synthetic K<sup>+</sup> ionophore depsipeptides and its implications in glucose-stimulated insulin secretion in  $\beta$ -Cells. *Chem.-Eur. J.* **2019**, *25*, 9287–9294.
- (38) Sanz-González, A.; Cózar-Castellano, I.; Broca, C.; Sabatier, J.; Acosta, G. A.; Royo, M.; Hernando-Muñoz, C.; Torroba, T.; Perdomo, G.; Merino, B. Pharmacological activation of insulin-degrading enzyme improves insulin secretion and glucose tolerance in diet-induced obese mice. *Diabetes Obes. Metab.* **2023**, *25*, 3268–3278.

- (39) Revilla-Cuesta, A.; Abajo-Cuadrado, I.; Medrano, M.; Salgado, M. M.; Avella, M.; Rodríguez, M. T.; García-Calvo, J.; Torroba, T. Silica Nanoparticle/Fluorescent Dye Assembly Capable of Ultra-sensitively Detecting Airborne Triacetone Triperoxide: Proof-of-Concept Detection of Improvised Explosive Devices in the Workroom. *ACS Appl. Mater. Interfaces* **2023**, *15*, 32024–32036.
- (40) Revilla-Cuesta, A.; Abajo-Cuadrado, I.; Medrano, M.; Salgado, M. M.; Pecori, G.; Rodríguez, T.; Hernando-Muñoz, C.; García-Calvo, J.; Arcos, J.; Torroba, T. New fluorescent reporters capable of ultra-sensitively detecting trinitrotoluene on surfaces: A proof-of-concept for finding hidden nitroaromatics in the workroom. *J. Photochem. Photobiol., A* **2023**, *444*, 114911.
- (41) Sanluis-Verdes, A.; Colomer-Vidal, P.; Rodríguez-Ventura, F.; Bello-Villarino, M.; Spinola-Amilibia, M.; Ruiz-Lopez, E.; Illanes-Vicioso, R.; Castroviejo, P.; Aiese Cigliano, R.; Montoya, M.; Falabella, P.; Pesquera, C.; Gonzalez-Legarreta, L.; Arias-Palomo, E.; Solà, M.; Torroba, T.; Arias, C. F.; Bertocchini, F. Wax worm saliva and the enzymes therein are the key to polyethylene degradation by *Galleria mellonella*. *Nat. Commun.* **2022**, *13*, 5568.
- (42) Spinola-Amilibia, M.; Illanes-Vicioso, R.; Ruiz-López, E.; Colomer-Vidal, P.; Rodríguez-Ventura, F.; Peces Pérez, R.; Arias, C. F.; Torroba, T.; Solà, M.; Arias-Palomo, E.; Bertocchini, F. Plastic degradation by insect hexamerins: Near-atomic resolution structures of the polyethylene-degrading proteins from the wax worm saliva. *Sci. Adv* **2023**, *9*, No. eadi6813.
- (43) Sun, L.; Liu, H.; Ye, Y.; Lei, Y.; Islam, R.; Tan, S.; Tong, R.; Miao, Y.-B.; Cai, L. Smart nanoparticles for cancer therapy. *Signal Transduct. Target. Ther.* **2023**, *8*, 418.
- (44) Beishenaliev, A.; Loke, Y. L.; Goh, S. J.; Geo, H. N.; Mugila, M.; Misran, M.; Chung, L. Y.; Kiew, L. V.; Roffler, S.; Teo, Y. Y. Bispecific antibodies for targeted delivery of anti-cancer therapeutic agents: A review. *J. Controlled Release* **2023**, *359*, 268–286.
- (45) Lammers, T. Nanomedicine Tumor Targeting. *Adv. Mater.* **2024**, *36*, 2312169.
- (46) García-Calvo, J.; Calvo-Gredilla, P.; Ibáñez-Llorente, M.; Romero, D. C.; Cuevas, J. V.; García-Herbosa, G.; Avella, M.; Torroba, T. Surface functionalized silica nanoparticles for the off-on fluorogenic detection of an improvised explosive, TATP, in a vapour flow. *J. Mater. Chem. A* **2018**, *6*, 4416–4423.
- (47) García-Calvo, J.; Robson, J. A.; Torroba, T.; Wilton-Ely, J. D. E. T. Synthesis and Application of Ruthenium(II) Alkenyl Complexes with Perylene Fluorophores for the Detection of Toxic Vapours and Gases. *Chem.-Eur. J.* **2019**, *25*, 14214–14222.
- (48) García-Calvo, V.; Cuevas, J. V.; Barbero, H.; Ferrero, S.; Álvarez, C. M.; González, J. A.; Díaz de Greñu, B.; García-Calvo, J.; Torroba, T. Synthesis of a Tetracorannulene-perylenediimide That Acts as a Selective Receptor for C60 over C70. *Org. Lett.* **2019**, *21*, 5803–5807.
- (49) Busto, N.; Calvo, P.; Santolaya, J.; Leal, J. M.; Guédin, A.; Barone, G.; Torroba, T.; Mergny, J.-L.; García, B. Fishing for G-Quadruplexes in Solution with a Perylene Diimide Derivative Labeled with Biotins. *Chem.-Eur. J.* **2018**, *24*, 11292–11296.
- (50) García-Calvo, J.; García-Calvo, V.; Vallejos, S.; García, F. C.; Avella, M.; García, J.-M.; Torroba, T. Surface Coating by Gold Nanoparticles on Functional Polymers: On-Demand Portable Catalysts for Suzuki Reactions. *ACS Appl. Mater. Interfaces* **2016**, *8*, 24999–25004.
- (51) Busto, N.; García-Calvo, J.; Cuevas, J. V.; Herrera, A.; Mergny, J.-L.; Pons, S.; Torroba, T.; García, B. Influence of core extension and side chain nature in targeting G-quadruplex structures with perylene monoimide derivatives. *Bioorg. Chem.* **2021**, *108*, 104660.
- (52) Revilla-Cuesta, A.; Abajo-Cuadrado, I.; Quadrini, L.; Failli, S.; Rodríguez-Rubio, A.; Cuevas, J. V.; Hernando-Muñoz, C.; García-Calvo, J.; Torroba, T. Chemical speciation of methylmercury and mercury(II) cations in fish by new fluorogenic naphthalimide alkynyl gold complexes: The ultimate test for detecting fish contamination. *Sens. Actuators, B* **2024**, *421*, 136492.
- (53) Frederix, P. W. J. M.; Patmanidis, I.; Marrink, S. J. Molecular simulations of self-assembling bio-inspired supramolecular systems and their connection to experiments. *Chem. Soc. Rev.* **2018**, *47* (10), 3470–3489.